

RECENT ADVANCES IN FLAME RETARDANT POLYMER NANOCOMPOSITES

Jeffrey W. Gilman^{1*}, Takashi Kashiwagi¹, Alexander B. Morgan¹,
Richard H. Harris Jr.¹, Lori Brassell¹, Walid H. Awad¹, Rick D. Davis²,
Leonard Chyall², Thomas Sutto³, Paul C. Trulove⁴, and Hugh DeLong⁵

¹ Building and Fire Research Laboratory,
National Institute of Standards and Technology, Gaithersburg, MD

² Great Lakes Chemical, West Lafayette, IL

³ Naval Research Laboratory, Washington, DC

⁴ Air Force Office of Scientific Research, Arlington, VA

⁵ Naval Academy, Annapolis, MD

INTRODUCTION

A new approach to address the ever increasing demand for higher performance flame retarded products has recently focused on use of mica-type clays nano-dispersed in commodity polymers. These “nanocomposites” exhibit the unusual combination of reduced flammability, in the form of lower peak heat release rates^(1,2,3,4), and improved physical properties? However, the details of the fire retardant mechanism are not well understood. In October of 1998 a NIST-industrial consortium was formed to study the flammability of these unique materials. The focus of research within this consortium was to develop a fundamental understanding of the fire retardant (FR) mechanism of polymer clay nanocomposites. We report here on some of the results of the first year of this study; we focus our discussions on the results for polystyrene (PS) a polymer system commonly used in flame retarded applications such as information technology (IT) equipment. The most important aspect of the nanocomposite approach is the combined improvement in both flammability properties and physical properties. However, methods for preparation, which supply fully optimized nanocomposites, are still under development. An important issue in this regard is processing stability of the treated clays. We also report on our recent efforts to address this issue through development of new thermally stable imidazolium-treated montmorillonite.

EXPERIMENTAL[‡]

Processing: PS-Nanocomposites. PS-nanocomposites were prepared by Great Lakes Chemical on a twin-screw extruder (25 mm, at 170°C). PS of two different M_n ⁶ (M_n 170,000, Styron 663 and M_n 100,000 XU70262.08) were compounded with quaternary alkylammonium treated montmorillonite (AMMT) from Southern Clay Products. Three PS/MMT formulations (2%⁷ AMMT, 5% AMMT, 10% AMMT) were prepared, for both M_n . All PS/MMT nanocomposites contained both intercalated MMT tactoids and delaminated single MMT layers, similar to nylon-nanocomposites prepared previously.⁴

[‡] The policy of the National Institute of Standards and Technology (NIST) is to use metric units of measurement in all its publications, and to provide statements of uncertainty for all original measurements. In this document however, data from organizations outside NIST are shown, which may include measurements in non-metric units or measurements without uncertainty statements. The identification of any commercial product or trade name does not imply endorsement or recommendation by the National Institute of Standards and Technology.

Characterization: The nanocomposite systems prepared were characterized using **X-ray** diffraction (XRD), and Transmission Electron Microscopy (**TEM**). XRD **data** were collected on a Phillips diffractometer using Cu K α radiation, ($\alpha=0.1505945$ nm). The d-spacing reproducibility is ± 0.06 nm (one sigma). **TEM** of PS-nanocomposite samples were prepared using room temperature ultramicrotomy to cut 70 nm thick sections. All sections were placed onto carbon-coated copper **grids**. Bright field **TEM** images were obtained at 120 kV, at low dose conditions, with a Phillips 400T, at magnifications of 2800, 28000, and 60000X. TEM negatives were then enlarged to 8400, 30000, 280000, and 600000X respectively to produce high magnification prints. The contrast between the layered silicates (clay) and the polymer phase **was** sufficient for imaging, **so** no heavy metal **staining** of sections prior to imaging **was** required.

Cone Calorimetry: Cone Calorimeter experiments were performed at an incident heat flux of 50 kW/m² using the cone heater? **Peak** heat release rate (HRR), **mass** loss rate (MLR), specific extinction area (SEA), ignition time (T_{ign}) carbon monoxide yield, carbon dioxide yield, and specific heat of combustion data are reproducible to within ± 10 % when measured at 50 kW/m² **flux**. The carbonaceous residue yields are reproducible to within ± 0.5 % (one sigma). The silicate fraction has been subtracted out of these **data**. The cone **data** reported here are the average of three replicated experiments. The specific errors (one sigma) are shown as error **bars** on the HRR plots.

Gasification: The detailed description of the gasification device built at **NIST** has been published previously.⁹ The gasification device allows pyrolysis, in a nitrogen atmosphere, of samples identical to **those used** in the Cone Calorimeter, without complications **from gas** phase combustion, such as heat feedback, **and** without obscuration of the sample surface **from** the flame. Typical measurements taken during a gasification experiment include **mass** loss rate (MLR), **and** video of the sample **as** it undergoes gasification. The gasification data reported here **are** the average of three replicated experiments. The specific errors (one sigma) are shown as error **bars** on the MLR plots.

UL-94 Flammability Test¹⁰ The UL-94 test is performed on a sample (125 mm by 13 mm, with **various** thickness up to 13 mm) suspended vertically above a cotton patch. The sample is subjected to two 10 s flame exposures with a calibrated flame in a **unit** which is **free from** the **effects** of external air currents. After the first 10 s exposure, the flame is removed, and the **time** for the sample to self-extinguish is recorded. **Cotton ignition** is noted if polymer dripping ensues; dripping is permissible if no cotton ignites. **Then** the second ignition is performed on the same sample, and the self-extinguishing time and dripping characteristics recorded. If the plastic self-extinguishes in less **than** 10 s after each ignition, with **no** dripping, it is classified as **V-0**. If it self-extinguishes in less than 30 s after each **ignition**, with no dripping, it is classified as a V-1, **and** if the cotton ignites then it is classified as V-2. If the sample **does** not self-extinguish before burning completely it is classified as failed (F).

Thermo-gravimetric analysis (TGA): TGA was carried out on polymer samples (5–10 mg) using a TA Instruments **SDT** 2960 Simultaneous DSC-TGA at 10 °C/min in nitrogen.

General Preparation of the substituted imidazolium salts: Imidazolium chloride salts. The alkyl chloride (1 mole), 1,2-dimethyl imidazole (0.95 mole) and acetonitrile (50 mL) were combined in a round bottom **flask** equipped with a reflux condenser. The mixture was refluxed for 7-10 days under **nitrogen**. After the reaction was complete, a large excess of ethyl acetate was added to precipitate the solid product. This solid was then filtered and washed several times with ethyl acetate to remove the 1,2-dimethyl imidazole. The resulting N-alkyl-1,2-dimethyl imidazolium chloride had residual solvent removed under vacuum, at 80 °C, for 12 hours. The solid was then re-dissolved in a minimum of acetonitrile and precipitated again with ethyl **acetate**. The white solid was then filtered and washed with ethyl acetate, **and** solvent removed under an active vacuum at 80

°C. N-alkyl-1,2-dimethyl imidazolium montmorillonites (IM-MMT). IM-MMT were prepared using standard ion exchange procedures for preparing organic treated montmorillonites.¹⁰

RESULTS AND DISCUSSION

Flammability Properties of PS nanocomposites: The heat release rate (HRR) data for the PS/MMT nanocomposites with 2 %, 5 %, and 10% AMMT are shown in Figure 1. The reduction in peak HRR improves as the mass fraction of MMT increases. The additional improvement for the PS/MMT nanocomposite with 10% **AMMT only** occurs during the first 100s of the burn. This is typical of the result for other polymer nanocomposites we evaluated. A leveling off of improvement in properties at 5 % is also a common result for many other properties (tensile strength, modulus, permeability, etc.). As impressive as the HRR data are for the PS system, the data most telling of the novelty of this approach, to flame retarding PS, comes **from** the gasification **data** taken on these samples.

Gasification of PS-clay nanocomposites. The nitrogen-gasification experiments allow pyrolysis of samples identical to those used in the Cone Calorimeter, without complications **from** gas phase combustion, such **as** heat feedback, and without obscuration of the sample surface **from** the flame. The gasification apparatus uses fire-like fluxes (25-75 kW/m²) similar to the Cone calorimeter. The combination of mass loss rate and video observations taken during gasification has proven invaluable to us in helping to understand condensed phase phenomena. The MLR **data** from the gasification of PS/MMT nanocomposites show the identical trends to those found in the HRR data from the Cone (see Figure 1). However, the digitized video images taken during the gasification of the low M_n PS/5 % MMT nanocomposite show the most important effect of the nano-dispersed clay on the PS degradation; in contrast to the rapidly-boiling liquid layer observed atop the pure PS, the PS/5 % **MMT** sample appears to solidify and converts to a black solid residue very early in the experiment, at 90 s. Once this residue (char) forms, the MLR slows to 25 % of that for pure PS. This is observed for both M_n of PS, except the high M_n PS nanocomposite intumesced to a greater extent than the low M_n PS nanocomposite during the charring process.

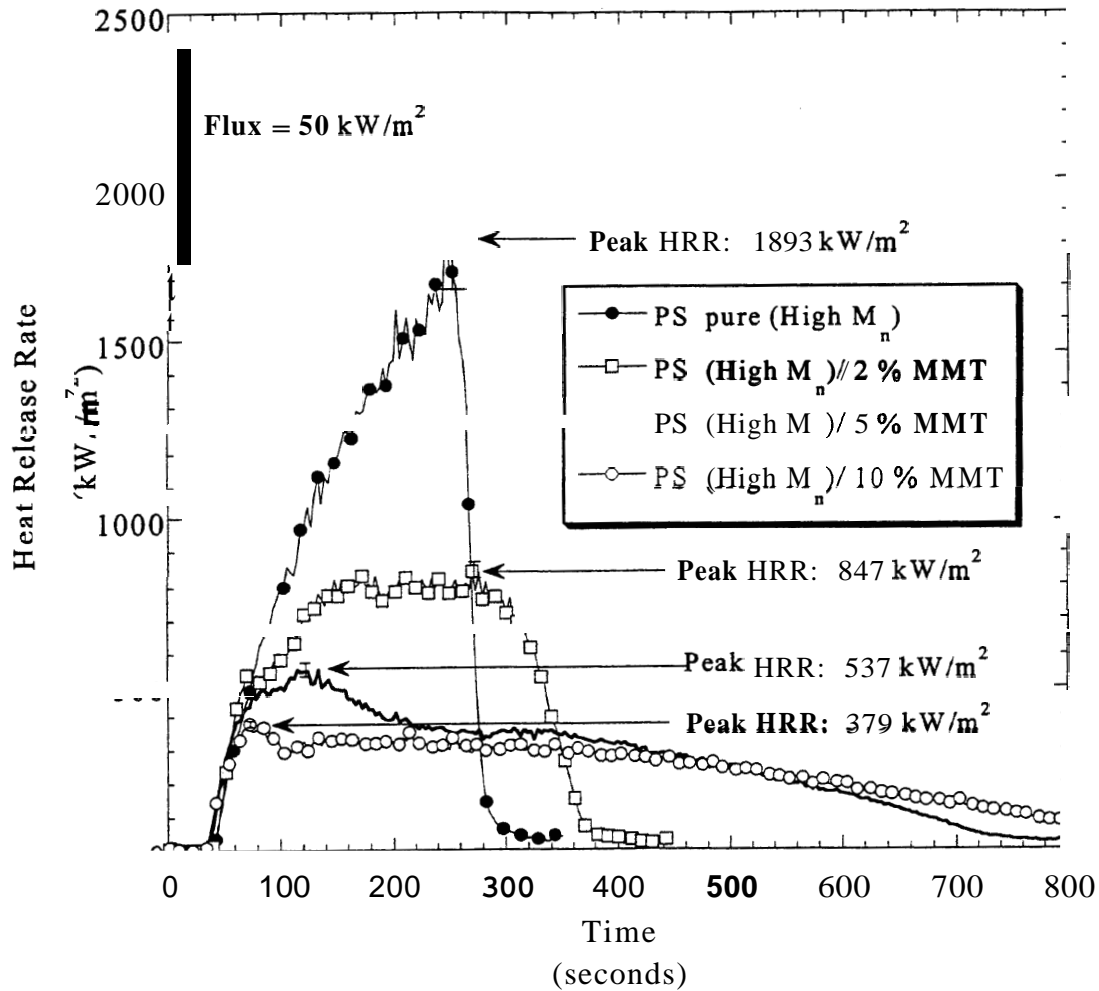


Figure 1. HRR plots for the pure high M_n PS, and the high M_n PS/ MMT nanocomposites with 2 %, 5 %, and 10% MMT .

This may indicate a higher melt viscosity for the sample that intumesced more, and suggests one reason that the decomposition products escaped the condensed phase at a slower rate (i.e., the MLR was lower for the high M_n PS nanocomposite). As stated before, it is this reduced MLR, or fuel feed rate, that is responsible for the dramatic reduction in the HRR. The data in Table 1 show that the MLR is the only flammability parameter which is significantly affected by the presence of nano-dispersed MMT.

	Residue Yield ^a [%]	Peak HRR [kW/m^2]	Average Specific Ext. Area [m^2/kg]	Average H_C [MJ/kg]	Peak MLR (Cone) [g/s]	Peak MLR (Gasification) [g/s]
PS (High M_n)	0.2 %	1870	1320	31	59	41

<i>PS/5 % MMT</i>	4.9 %	540	1230	26	22	14
PS (Low M_n)	0.3 %	1940	1300	31	63	42
<i>PS/5 % MMT</i>	4.9 %	540	1650	29	19	13

The video images (Figure 2) and the gasification residue yield data (Table 2) for the PS/MMT nanocomposites show that the otherwise non-char forming PS is converted to a charring system by the nano-dispersed clay. This is significant because very few other additive flame retardants are capable of causing virgin PS (without a carbonific) to give carbonaceous char, especially at this low a loading, and with such dramatic reduction in flammability.

Table 2. Carbonaceous char yields for PS/MMT nanocomposites.

Nanocomposite	Carbonaceous Char yield ^a
PS/2 % AMMT	0.7 %
PS/5 % AMMT	2.3 %
PS/10 % AMMT	3.3 %

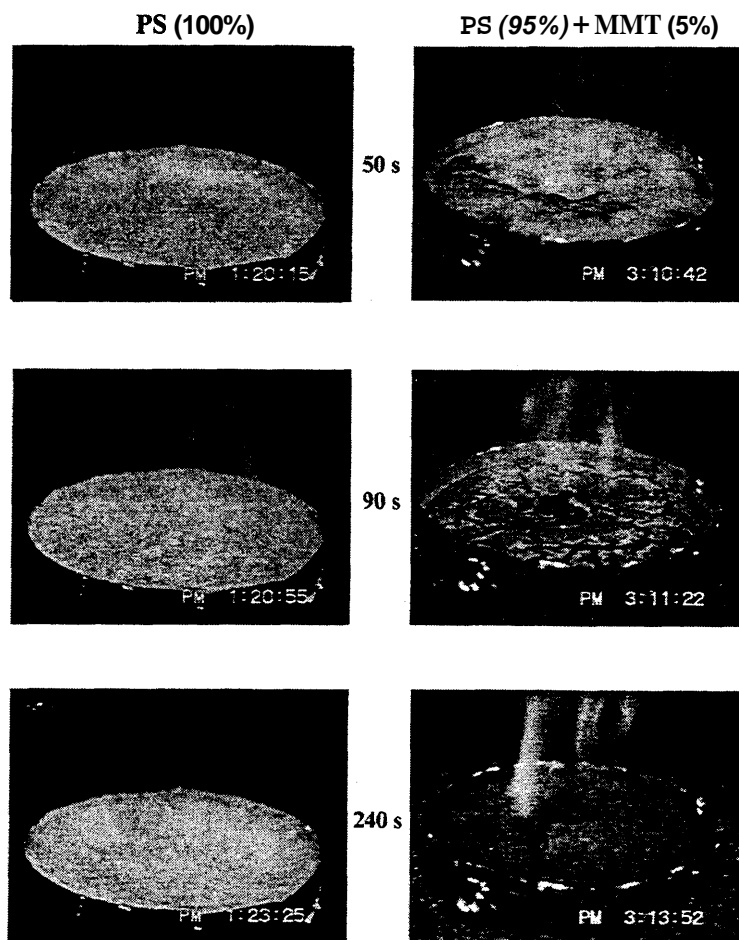


Figure 2. Digitized images from nitrogen gasification at a flux of 50 kW/m^2 of pure PS (low M_n) and PS/5 % MMT nanocomposite (low M_n).

Organo-modified Montmorillonite: The processing stability of the polymer and the organo-clay used to prepare the nanocomposite has a significant influence on the flammability performance of nanocomposites. In a previous TGA-FTIR study, of the pyrolysis of PS/MMT nanocomposites, aliphatic decomposition products were observed before the onset of PS degradation, indicating the organic treatment in the MMT was degrading at a lower temperature than the PS.³ GPC analysis of the extruded PS nanocomposite samples (see Figure 3) reveals some evidence of degradation, in the form of lower M_w .⁴ Finally, since the molecular weight degradation only occurs if quaternary alkylammonium-MMT is present, and does not occur, either if pure polymer is extruded, or if the PS is extruded with sodium montmorillonite (NaMMT), it appears that the presence of the quaternary alkylammonium, in the MMT, somehow contributes to the degradation of the PS also. This degradation is of particular concern since we have found that, when extensive degradation occurs, the flame retardant effect is completely **negated**.⁴ In addition, this could also limit the improvements in other physical properties observed for PS/MMT nanocomposites.

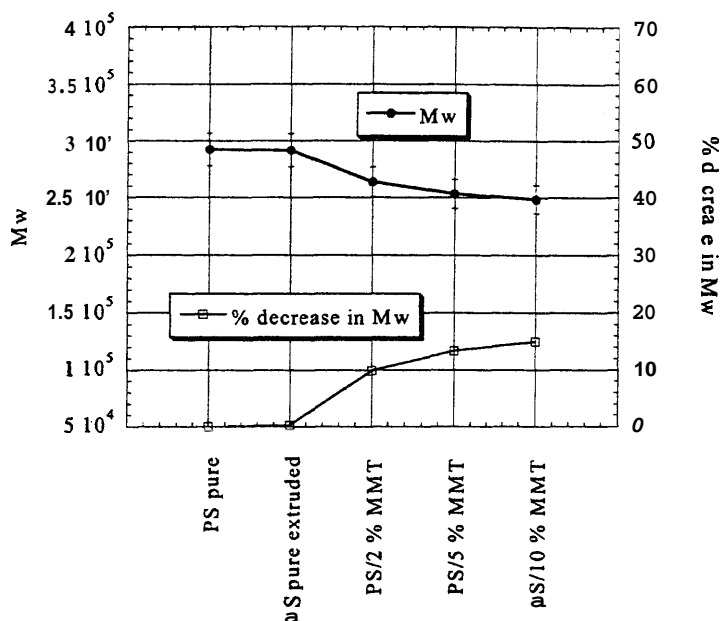


Figure 3. GPC data for high Mn PS and PS/5 % MMT nanocomposites. Significant loss of M_w is evident at all concentrations of AMMT. Standard uncertainty in the M_w data is shown as an error bar in the plot.

High melt-temperature engineering polymers, such as Nylon-6 and polycarbonate, raise additional concerns when considering preparation of nanocomposites by melt extrusion, or processing (injection molding) of the nanocomposites into final molded products. The problem is that most alkyl ammonium treatments for MMT have an onset of thermal decomposition at about 200 °C. To facilitate rapid manufacturing, typical industrial melt-processing temperatures, of Nylon-6 for example, are in excess of 300 °C.¹¹ The issue is whether, or not, the alkyl ammonium treated MMT can survive short residence times (<200 sec) in high-shear environment in the extruder at 300 °C.

However, we recently found that degradation of quaternary alkyl ammonium treated MMT occurs during melt extrusion of Nylon-6/AMMT. The samples evaluated were from a study that examined the role of processing conditions (twin-screw: shear and design) in determining the optimal circumstances for preparing Nylon-6/MMT nanocomposites.¹² The NMR data of Nylon-6/AMMT samples treated with dimethyl, di(hydrogenated tallow) ammonium ion, showed significant concentrations of tertiary amine after extrusion. The concentration of tertiary amine was directly proportional to the residence time in the extruder, and appears to be independent of the thermal history in the absence of shear. It was found that as much as 80 % (± 10 %) of the quaternary alkylammonium had degraded in the samples with extrusion residence times long enough to give delaminated nanocomposites.¹³ A comparison of another delaminated nylon-6/MMT nanocomposites from the same study, prepared using dihydroxyethyl, hydrogenated tallow ammonium/MMT, which showed an order-of-magnitude less degradation of the organic treatment, revealed inferior mechanical properties for the degraded nylon-6/MMT nanocomposite.¹² We have also found significantly higher concentration of caprolactam monomer in Nylon-6/MMT nanocomposite injection molded at 300 °C.¹⁴ In light of these results we have focused our efforts on development of organic treatments for MMT and other nano-additives with improved processing stability.

Imidazolium and Crown ether treated Montmorillonite. We decided to focus on imidazolium salts, since it has been reported that the delocalized imidazolium cation has better thermal stability than the alkyl ammonium cation.¹⁵ Imidazolium salts shown in Figure 4 were used to treat NaMMT, via standard literature ion exchange methods, to give a series of imidazolium-MMT (IM-MMT). For our second approach we selected crown-ethers; because of the strong binding capacity they have for cations, such as the sodium cation in NaMMT, and the good solubility the resulting complexes have in organic solvents. Crown ether treatment of NaMMT organically modifies the clay but leaves the sodium cation in the gallery. We added 18-crown-6 to NaMMT in solution to give a 18-crown-6 Na⁺ MMT complex (Figure 5) (18c6-NaMMT). The modified clays, 18c6-NaMMT, and several IM-MMT were analyzed by XRD to determine if the spacing between the clay layers (d-spacing) had changed. The XRD data showed that the d-spacing for 18c6-NaMMT increased by 0.24 nm. We also observed the expected increase in layer (d) spacing as the R-group on the imidazolium increased in length within the series of MMT-derivatives prepared (see Figure 6).

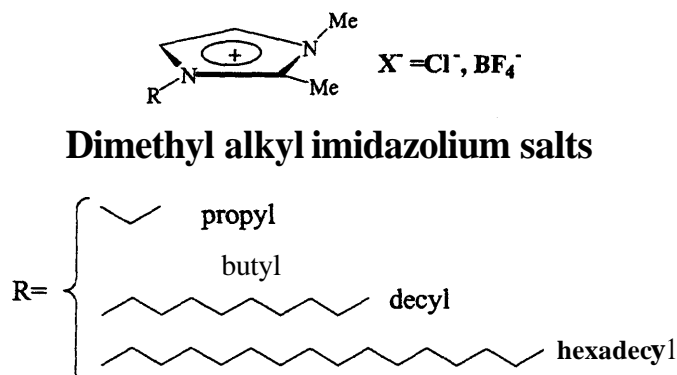


Figure 4. Structures of various imidazolium salts used to treat sodium montmorillonite.

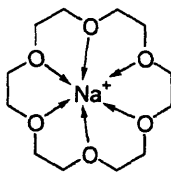


Figure 5. 18-crown-6Na⁺ complex.

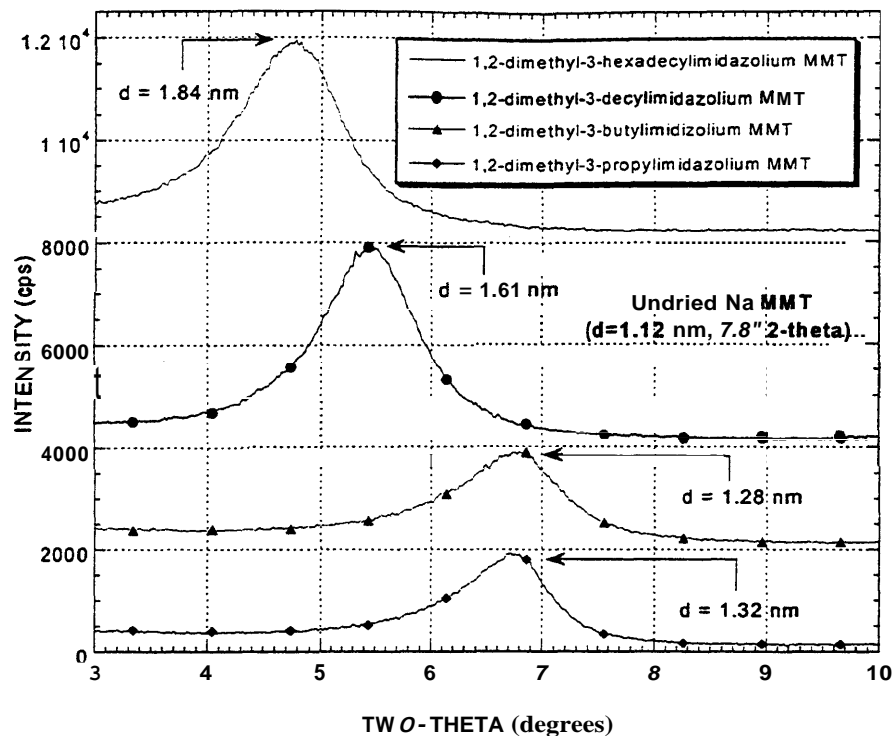


Figure 6. XRD data for several IM-MMT salts showing the d-spacing between MMT layers. The d-spacing increases as the R-group size increases in length from butyl to decyl to hexadecyl. The d-spacing reproducibility is ± 0.06 nm (one sigma).

Since the thermal stability of the organic treatment of the clay is of prime importance, thermogravimetric analysis (TGA) was carried out on these materials. For comparison, we also analyzed the quaternary alkyl ammonium treated clay (AMMT) discussed above. [Recall that AMMT is montmorillonite treated with dimethyl bis(hydrogenated tallow) ammonium.] The TGA data summarized in Table 3, for the imidazolium, crown ether and quaternary alkylammonium treated montmorillonite samples, clearly show the improvements in thermal stability for 18c6-NaMMT and all of the IM-MMT compared to AMMT.

Table 3. Thermal stability data for imidazolium, crown ether and quaternary alkyl ammonium treated montmorillonite.

Sample	Onset - T_{dec} °C	Peak - T_{dec} (dTGA) °C
1,2-dimethyl-3-N-hexadecyl imidazolium/MMT ¹	287	375
1,2-dimethyl-3-N-hexadecyl imidazolium/MMT ²	275	400
1,2-dimethyl-3-N-decyl imidazolium/MMT	267	443
1,2-dimethyl-3-N-butyl imidazolium/MMT	305	445
18-Crown-6/NaMMT	300	390
dimethyl-di(hydrogenated tallow) ammonium/MMT	200	310

2: prepared using 1,2-dimethyl-3-N-hexadecyl imidazolium Cl salt
Repeatability of onset and peak T_{dec} measurements are ± 0.6 °C

While the improved thermal stability is of key importance to making polymer-clay nanocomposites, the organically treated clay must also be compatible with the polymeric matrix, monomer, or solvent; otherwise the material will not disperse in the polymer during processing to form a

nanocomposite. Two of the new modified-MMT materials, **18-Crown-6/NaMMT** and 1,2-dimethyl-3-N-hexadecyl imidazolium/MMT (DMHDIM-MMT) were blended with Nylon-6 and PS, respectively, using a lab-scale micro twin screw extruder.

XRD of the **18-Crown-6/NaMMT/Nylon-6** blend shows no peaks in the low angle region, indicating a disordered system. Transmission electron microscopy (TEM) analysis shows that the MMT was well dispersed throughout the polymer (Figure 7).



Figure 7. **TEM** image of Nylon-6 with 10% 18-crown-6/NaMMT nanocomposite.

However, some large multi-layer stacks or tactoids remain, but small 3-7 layer tactoids predominate. Since no d-spacing can be obtained from the XRD data, it cannot be determined whether these tactoids are intercalated or not. NaMMT, however, does not disperse well in nylon-6,¹⁶ therefore it appears that the **18-crown-6/NaMMT** gallery is sufficiently hydrophobic to be compatible with the nylon-6 and gives a well-dispersed nanocomposite. Possibly, modification of the NaMMT **with** a more organophilic crown ether would be even more effective, and we are exploring this issue.

XRD of **1,2-dimethyl-3-N-hexadecyl** imidazolium/5 % MMT/PS also produced no peaks in the low angle region. This sample is currently being further characterized using TEM and NMR. Preliminary TGA **data** show that this sample has **40 °C** better thermal stability, **as** measured by the onset of decomposition, compared to pure PS.

SUMMARY

The most important aspect of the nanocomposite approach is the combined improvement in **both** flammability properties and physical properties. We have found that nano-dispersed montmorillonite causes non-char forming polymers, such as polystyrene, to form char. The resulting residue is essentially a carbonaceous-silicate nanocomposite, where the clay enhances the insulating and mass transport properties of the carbonaceous char, **and** provides the flame retardant

effect. However, the enhanced physical and flammability properties of the nanocomposite may be counteracted by processing degradation of the polymer and, or the organic-treated montmorillonite. One solution to these issues is development of organic treatments for the montmorillonite with improved processing stability. The two new organic treatments highlighted here, imidazolium cations and crown ethers, show promise towards meeting this goal. Efforts are currently underway in our laboratory to optimize these treatments for use with montmorillonite and other nano-additives to prepare a variety of flame retarded polymer- nanocomposites. Once these new approaches are optimized and fully characterized, their flammability and physical properties will be evaluated to determine if they offer the processing stability and optimal properties envisioned.

Acknowledgments. The authors wish to thank the following members of NIST-Materials Science and Engineering Laboratory: Dr. Alan Nakatani for assistance in use of the micro twin-screw extruder, Dr. Catheryn Jackson for TEM assistance, and Dr. James Cline for use of XRD facilities. We also want to thank Southern Clay Products for the donation of MMT samples and technical assistance in preparing the organically treated clays. Finally, we wish to thank the following organizations for funding of this work: Air Force Office of Scientific Research, Federal Aviation Administration (DTFA 03-99-X-9009) and the Flammability of Polymer-Clay Nanocomposites Consortium.

-
1. Gilman, J. W.; Kashiwagi, T.; Lichtenhan, J. D. *SAMPE Journal*, **1997**, *33*, 40.
 2. Gilman, J. W.; Kashiwagi, T.; Lomakin, S.; Giannelis, E.; Manias, E.; Lichtenhan, J.; Jones, P. in *Fire Retardancy of Polymers: the Use of Intumescence*. The Royal Society of Chemistry, Cambridge, **1998**, 203-221.
 3. Gilman, J. W. *App. Clay. Sci.* **1999**, *15*, 31.
 4. Gilman, J. W.; Jackson, C. L.; Morgan, A. B.; Harris, R. H.; Manias, E.; Giannelis, E. P.; Wuthenow, M.; Hilton, D.; Phillips, S. *Chem. Mater.* **2000**, *12*, 1866.
 5. Giannelis, E., *Advanced Materials* **1996**, *8*, 29.
 6. According to ISO 31-8, the term "Molecular Weight" has been replaced by "Relative Molecular Mass", symbol M_r . Thus, if this nomenclature and notation were used here, $M_{r,n}$ instead of the historically conventional M_n for the average molecular weight (with similar notation for M_w , M_z , M_v) would be used. It would be called the "Number Average Relative Molecular Mass". The conventional notation, rather than the ISO notation, has been employed here.
 7. Percent (%) denotes mass fraction percent in all formulations.
 8. Babrauskas, V., *Fire and Materials*, **1995**, *19*, 243.
 9. Austin, P. J., Buch, R. B., Kashiwagi, T. *Fire and Mater.*, **1998**, *22*, 221.
 10. Vaia, R., A., Teukolsky, R., K., and Giannelis, E. P. *Chem. Mater.* **1994**, *6*, 1017-1022.
 11. Hughes, K.; Bohan, J.; Jay, T.; Prins, A. *Proceeding of Flame Retardants Chemical Assoc. Meeting, March 2000*, 85-89.
 12. Dennis, H. R., Hunter, D. L., Chang, D., Kim, S., White, J. L., Cho, J. W., and Paul, D. P. *Proceedings of ANTEC 2000*, 2000, Orlando, May.
 13. VanderHart, D. L., Asano, A., and Gilman, J. W. *Macromol.* Submitted.
 14. Davis, R., VanderHart, D. L., Asano, A., and Gilman, J. W., manuscript in preparation.
 15. Ngo, H., L., LeCompte, K., Hargens, L., McEwen, A., B. *Thermochemica Acta*, **2000**, 357-358, 97.
 16. Maxfield, M; Christiani, B. R.; Murthy, S. N.; Tuller, H. US patent 5,385,776. Issued to Allied Signal, Inc., 1995.